SECOND-ORDER WAVE LOADS ON A STATIONARY BODY

By

C.-H. Lee
Department of Ocean Engineering, MIT
Cambridge, MA 02139, USA

(Abstract for the 6th International Workshop on Water Waves and Floating Bodies, April 1991)

Introduction

Second-order wave effects are important to the dynamics of a certain type of offshore structures and marine vessels. They are known to excite the resonant motions of the structures whose natural frequencies are designed to lie outside the spectral range of wave incounter. The high frequency vertical plane resonance of the TLP and the low frequency large amplitude oscillation of compliant floating structures are the well known examples. In the past decade numerous research efforts devoted to the analysis and computation of second-order wave effects. Recently we developed a numerical method and extended the first order panel code (Korsmeyer et al (1988)) for the computation of complete second order sum and difference-frequency wave forces on the arbitrary three dimensional bodies in the presence of bichromatic and bidirectional waves. Detailed description of the second-order extension can be found in Lee et al (1991). Much efforts are directed to the robust and efficient evaluation of slowly convergent free-surface integral associated with the free-surface boundary condition.

Formulation

With the assumptions of a potential flow and weak nonlinearity, the velocity potential $\Phi(\mathbf{x},t)$ and resultant force $\mathbf{F}$ can be expanded in terms of first-order linear components and second-order components. Here $\mathbf{x}$ is a fixed Cartesian coordinate system, and t denotes time. Unlike its first-order counterpart the boundary value problem for second-order potential is characterized by an inhomogeneous free surface boundary condition, involving quadratic products of the linear velocity potential and its spatial derivatives. In the presence of two incident waves of frequencies ω_i and ω_j the second-order potential, which results from the quadratic interaction among first-order quantities, is given by

$$\Phi^{(2)}(\mathbf{x},t) = \mathrm{Re}\sum_i \sum_j \{\phi_{ij}^+(\mathbf{x})e^{i(\omega_i+\omega_j)t} + \phi_{ij}^-(\mathbf{x})e^{i(\omega_i-\omega_j)t}\} \tag{1}$$

Here $(+)$ and $(-)$ denote sum and difference-frequency components, respecively. A similar decomposition applies to the resultant force and we define the second-order force in the form

$$\mathbf{F}^{(2)}(t) = \mathrm{Re}\sum\sum\{\mathbf{F}_{ij}^+ e^{i(\omega_i+\omega_j)t} + \mathbf{F}_{ij}^- e^{i(\omega_i-\omega_j)t}\} \tag{2}$$

Two separate components contribute to $\mathbf{F}_{ij}$ as

$$\mathbf{F}_{ij} = \mathbf{F}_p + \mathbf{F}_q \tag{3}$$

where $\mathbf{F}_p$ is due to the $\Phi^{(2)}$ and $\mathbf{F}_q$ is due to the quadratic interactions of the linear potential $\Phi^{(1)}$.

Numerical method

• Quadratic force

For the diffraction problem there are no body motions, and the second-order force $\mathbf{F}_q$ takes the relatively simple form

$$\mathbf{F}_q = \frac{1}{2}\rho g \int_{WL} \mathbf{n}\zeta^2(1-n_z^2)^{-\frac{1}{2}}dl - \frac{1}{2}\rho \iint_{S_B} \mathbf{n}\nabla\Phi^{(1)}\cdot\nabla\Phi^{(1)}dS \tag{4}$$

Here ρ is the fluid density, g is gravity, n is the normal vector, ζ is the first-order runup and WL represents the waterline.

Robust evaluation of the first-order velocity $\nabla\Phi^{(1)}$ is essential to the reliable computation of (4). For this reason, the source-base formulation is used to evaluate the gradient in (4). (The advantage of the source formulation in this context is that the gradient of the source distribution requires only first derivatives of the Green function, whereas in the potential formulation second derivatives result from the gradient of the normal dipoles.) In addition special care is devoted to the discretization near the corners with a nonuniform spacing of the panels according to the 'cosine-spacing' formula or a similar scheme.

• Second order potential force

Indirect method which does not require the second-order potential explicitly is adopted in the computation of second-order potential force in consideration of the compatibility of the architecture of the second order code with that of the first-order code. The second-order force $\mathbf{F}_p$ is given by

$$\mathbf{F}_p = -i\rho\omega^{\pm}\iint_{S_B}(\phi_I\mathbf{n} - \psi\frac{\partial\phi_I}{\partial n})dS - i\rho\omega\iint_{S_F} q_F\psi dS. \tag{5}$$

where ϕ_I and ψ are second-order incident velocity potential and assisting potential. The free-surface forcing is denoted by q_F.

The second integral over the free surface S_F is the most difficult and computationally dominant task. For the efficient evaluation of this integral, the free surface S_F is divided in two parts, separated by a 'partition' circle of radius b which is sufficiently large to enclose the body and its local disturbance.

In the inner region between the body and the partition circle the free surface is discretized into quadrilateral panels to permit the free-surface integral to be evaluated by quadratures from the value of the integrand at each panel centroid. Terms in q_F containing second derivatives with respect to z cause numerical problems in the vicinity of the body waterlines. To avoid this, an alternative formulation involving only first-order spatial derivatives is used. Details can be found in Kim (1990).

In the outer region of the free surface ($r > b$) both the assisting potential and the first-order potentials can be expanded in Fourier-Bessel series. After integrating the trigonometric functions with respect to the angular coordinate the free-surface integrals are reduced to summations of integrals (with respect to the radial coordinate r) of the form

$$\int_b^{\infty} C_l(k_i r)C_m(k_j r)C_n(k_k r)rdr \tag{6}$$

Here the functions C_ν denote Hankel functions of the first or second kind ($H_\nu^{(1,2)}$), and Bessel functions of the first kind (J_ν). The arguments of these functions are proportional to the wavenumbers (k_i, k_j) corresponding to the first-order frequencies ω_i, ω_j, as well as the wavenumber k_k of the second-order potential or assisting potential. The neglected evanescent terms are local and decay exponentially to the radial direction in a fluid of finite depth. For large values of r/h, where h is the depth the evanescent modes are proportional to the factor $\exp(-Cr/h)$ where $\pi/2 < C < \pi$. If the partition radius is substantially larger than the fluid depth the resulting error is extremely small. On the other hand, in the infinite-depth limit the evanescent modes decay algebraically in proportion to $(kr)^{-3}$ on the free surface.

Special care is required to evaluate the radial integrals (6) in a robust manner for the relevant combinations of the wavenumbers and orders (ℓ, m, n). The maximum value of orders ℓ, m, n depends on the wavenumbers, body dimension and the partition radius. For the sum-frequency results presented, it is necessary to include orders up to a maximum value between 16 and 32. The method used for the evaluation of (6) is based on adaptive numerical integration in the complex plane, ultimately along a semi-infinite path parallel to the imaginary axis where the integrand decays exponentially with monotonic asymptotic form. Romberg quadratures are used for each of the required integrals, with a specified absolute error tolerance (generally 10^{-3}). Effective evaluation of the integrand (the Bessel and Hankel functions) is important in this method. For each combination of frequencies the total number of integrals (6) evaluated is O(1000), but the resulting computational burden is negligible compared to the numerical integration required for inner region of the free surface.

Numerical results and Disscusion

Computation was made for the wave loads on the single and four cylinders and ISSC TLP. The dominant effects of the second-order potential force to the vertical force and pitch moments at the sum-frequency are illustrated in the Figure. It is also found that second-order forces are much effected by multi-body interaction effects. In Table the comparison of second-order forces is shown between deep and shollow water as the partion radius changed. It is found that free-surface discretization is critical, particularly for the sum-frequency vertical force in deep water.

Acknowledgement

This work was conducted under the first and second Joint Industry Projects.

Reference

Kim, M.-H. 1990 'Second-order sum-frequency wave loads on large-volume structures,' *App. Ocean Research*, to appear.

Korsmeyer, F. T., Lee, C.-H., Newman, J. N., & Sclavounos, P. D. 1988 'The analysis of wave interactions with tension leg platforms,' OMAE Conference, Houston.

Lee, C.-H., Newman, J.N., Kim M.-H. & Yue D.K.P. 1991 'The computation of second-order wave loads', Submitted to OMAE.

Partition Radius:		112m	120m	140m	160m	180m	200m
Free-Surface Panels:		4928	6368	9728	13568	17888	22688
ka	Mode						
	3	2.25	2.32	2.34	2.38	2.39	2.40
0.545	1	7.89	7.98	8.05	8.12	8.15	8.15
	5	7.23	7.23	7.25	7.27	7.28	7.28
	3	3.83	3.95	3.99	4.05	4.07	4.08
0.845	1	11.82	12.07	12.11	12.21	12.26	12.27
	5	14.09	14.14	14.17	14.20	14.22	14.22
	3	3.63	3.76	3.82	3.88	3.91	3.92
1.220	1	14.46	14.64	14.60	14.64	14.73	14.64
	5	12.12	12.28	12.32	12.37	12.43	12.43
	3	0.53	0.58	0.66	0.72	0.77	0.80
0.545	1	7.00	7.05	7.17	7.24	7.27	7.28
	5	9.46	9.41	9.31	9.24	9.19	9.14
	3	1.85	1.89	1.95	2.01	2.05	2.09
0.845	1	10.70	10.89	11.10	11.19	11.24	11.27
	5	16.91	16.91	16.80	16.70	16.61	16.55
	3	0.67	0.54	0.34	0.28	0.28	0.31
1.220	1	13.49	13.61	13.78	13.81	13.91	13.80
	5	16.35	16.44	16.42	16.33	16.29	16.23

Table – Convergence of the second-order potential forces with increasing partition radius. Upper half of table is for a depth of 40m, and lower half is for a depth of 450m.

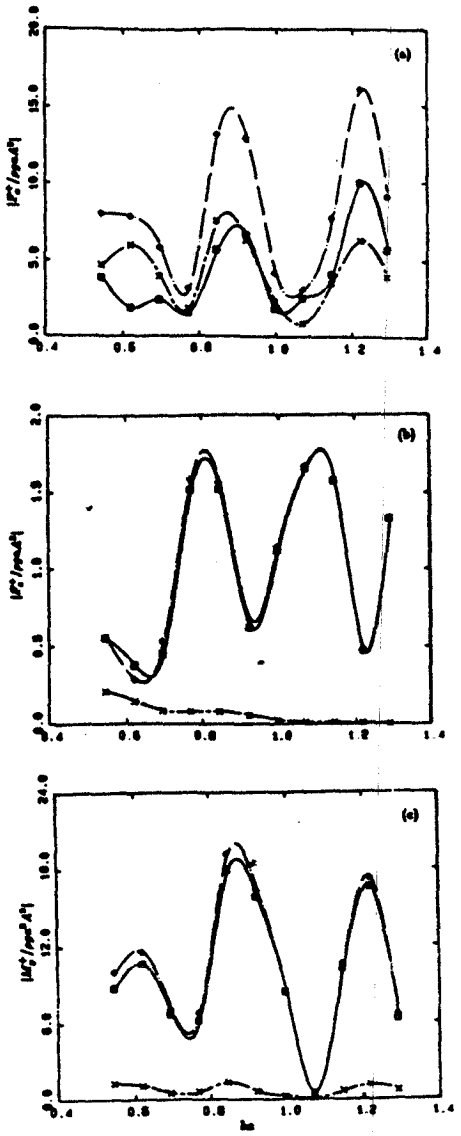

Figure – Amplitudes of the second-harmonic surge force (a), heave force (b), and pitch moment (c), as functions of the nondimensional incident wavenumber ka. The forces are nondimensionalized by the factor $\rho g a A^2$, and the moment by $\rho g a^2 A^2$, where ρ is the fluid density, g gravity, $a = 8.425$m the radius of the columns, and A the (first-order) incident wave amplitude. Separate contributions are shown from the second-order potential force F_p (o), quadratic force F_q (×), and the total force (□).

Sebastiani: We developed a similar procedure, which we presented at the last IUTAM Symposium. We also encountered the numerical difficulties of calculating double derivatives on the free surface, as well as, integrals of triple products of Bessel functions in the outer domain. In order not to increase the number of integrals, we directly computed the double derivatives using a low order panel method. We found the application of Romberg quadrature to the Bessel integrals troublesome, and preferred to use the asymptotic expansion of the Bessel functions. This leads to Fourier integrals which are easily evaluated.

Lee: Using a low order panel method the double spacial derivative can not be evaluated accurately (even approximately) close to the body surface, especially when the field point approaches the panel edge as required in the free surface integral near the waterline in the inner domain. The free surface integral can be converted, by applying the divergence theorem, into an integral involving only first order derivatives and by employing a source formulation this integral is evaluated accurately. The additional line integral along the waterline and the partition circle resulting from the divergence theorem can be evaluated with very small additional effort. In the outer domain, we didn't encounter any trouble in applying adaptive Romberg quadrature in the complex plane. Using the asymptotic expansion of the Hankel function may be complicated since the expansion is not uniform and the number of terms in the expansion depends on the order of the Hankel function as well as the partition radius. The numerical effort associated with the Romberg quadrature turned out to be very small compared to that of the 2D surface integral in the inner domain.

Molin: I refer to your table showing the convergence of the free surface integral with increasing radius of the partition circle. Do you have any explanation for the decrease in the heave force with increasing radius in the case $ka = 1.22, h = 450$, whereas the other forces increase? (From my experience it always increases at large wave numbers where the evanescent modes dominate).

Lee: I do not have an explanation for the decreasing value of the heave force. It is not clear to me why the force should vary monotonically with the increasing partition radius. It may depend not only on the magnitude but also on the phase of the free surface integral. In the table, for this particular frequency, the heave force happens to be very small compared to the other forces. Due to cancellation error, it may not represent a typical (correct) trend of heave forces especially for large partition radius.